EUROPEAN ORGANIZATION FOR NUCLEAR RESEARCH

CERN/EP 88-10
26 January 1988

RAPIDITY DEPENDENCE OF MULTIPLICITY DISTRIBUTIONS IN PROTON-NUCLEUS COLLISIONS AT 360 GeV/c

EHS - RCBC Collaboration

J.L.Bailly[9], S.Banerjee[1], C.Caso[5], Y.Chiba[7d], H.Dibon[12], B.Epp[6], A.Ferrando[8], F.Fontanelli[5], T.Gemesy[2], A.Gurtu[1], R.Hamatsu[7a], T.Hirose[7a], J.Hrubec[12], Y.Iga[7a], Yu.Ivanyshenkov[11], N.Khalatyan[11], E.Kistenev[11], S.Kitamura[7a], V.Kubik[11], J.MacNaughton[12], S.Matsumoto[7c], I.S.Mittra[4], L.Montanet[3], G.Neuhofer[3], G.Pinter[2], P.Porth[12], T.Rodrigo[8], J.Singh[4], S.Squarcia[5], K.Takahashi[7b], L.A.Tikhonova[10], U.Trevisan[5], T.Yamagata[7a], G.Zholobov[11], S.A.Zotkin[10]

1 Tata Institute of Fundamental Research, 400005 Bombay, India
2 Central Research Institute for Physics, H-1525 Budapest 114, Hungary
3 CERN, European Organization for Nuclear Research, CH-1211 Geneva 23, Switzerland
4 Panjab University, 160014 Chandigarh, India
5 University of Genova and INFN, I-16146 Genova, Italy
6 Institut für ExperimentalPhysik, A-6020 Innsbruck, Austria
7a Tokyo Metropolitan University, 158 Tokyo, Japan
7b Tokyo University of Agriculture and Technology, 184 Tokyo, Japan
7c Chuo University, Tokyo, Japan
7d Hiroshima University, 730 Hiroshima, Japan
8 Centro de Investigaciones Energéticas, Medioambientales y Tecnológicas, Madrid 28040, Spain
9 Université de l'Etat, Faculté des Sciences, B-7000 Mons, Belgium
10 Moscow State University, SU-117234 Moscow, USSR
11 Institute for High Energy Physics, Serpukhov, SU-142284 Protvino, USSR
12 Institut für Hochenergiephysik, A-1050 Wien, Austria

Submitted to Zeitschrift für Physik C

Abstract

Multiplicity distributions in various rapidity intervals for all charged particles produced in collisions of 360 GeV/c protons with aluminium (Al) and gold (Au) targets are presented. The data were analysed separately for the forward and backward hemispheres. Each distribution is well described by a negative binomial distribution. The experimental distributions are compared with the predictions of the multi-chain model calculated by the Monte Carlo program MCMHA in which the intranuclear cascade process is included, and also with the Lund Monte Carlo FRITIOF. The results of MCMHA reproduce quite well the multiplicity distributions for various rapidity intervals.

1. Introduction

Multiplicity distributions P(n) of charged particles have been studied in detail in experiments with hadron and lepton beams at center of mass energies up to 900 GeV [1-4]. These measurements have provided important constraints for mechanisms of multiparticle production. Several phenomenological models have been proposed to parameterise multiplicity distributions [1,5-8]. Recently the UA5 collaboration [1] has found that the charged multiplicity distribution can be described with a negative binomial distribution (NBD). It was shown that the NBD describes quite well the multiplicity not only of all charged particles produced in the full phase space, but also of those produced in the limited pseudorapidity regions.

The NBD is given by the following form:

$$P(n;k,\bar{n}) = \frac{k(k-1)....(k+n-1)}{n!} \left(\frac{\bar{n}}{\bar{n}+k}\right)^{n} \left(\frac{k}{\bar{n}+k}\right)^{k} \qquad (1)$$

where k and $\bar{n}$ are free parameters. The average multiplicity $\langle n \rangle$ and the dispersion D are related to the NBD parameters as follows:

$$\langle n \rangle = \bar{n}$$
$$D^2 = \bar{n} + \bar{n}^2/k \qquad (2)$$

After the original observation of the UA5 collaboration, similar analyses have been performed for hadron-hadron collisions [2], for e^+e^- annihilation [3] and for lepton-hadron scattering [4], and have shown that their charged multiplicity distributions in various rapidity intervals follow an NBD.

Several models have been put forward in order to interpret these experimental results. In the clan model [9] particle production can be explained in terms of stimulated emissions, or of cascading decays via independent clusters (clans). The NBD rule may hold for other interpretations [10-12]. The dependence of the NBD parameters on energy and rapidity interval, has also been discussed previously [1,12-13].

It has been found for interactions of 200 GeV/c protons with argon and xenon nuclei [14] that the charged multiplicity distributions in selected rapidity regions follow an NBD. It is interesting that the multiplicity distributions of hadron-nucleus interactions, considered as multiple collisions between a projectile and nucleons in a target nucleus, are also described by the NBD as well as those of the elementary particle interactions, i.e. hadron-hadron, e^+e^- and lepton-hadron collisions. This analysis has shown clear differences in the behaviour of the NBD parameters between the forward and backward hemispheres. An A-dependence of the parameters has also been observed. Results of this analysis were interpreted in the framework of the clan model [8] and one could observe that the absolute number of "clans" for p-nucleus collisions turns out to be significantly smaller in the backward than in the forward hemisphere, in particular for large rapidity intervals.

In our previous paper [15], we have found that multiplicity distributions of shower particles show a deviation from the universal KNO scaling curve when the target mass number is increased. The experimental data were well described in the whole rapidity range by Monte Carlo calculations [16-17] based on

the multi-chain model [18]. This calculation takes into account properly the formation zone concept and the intranuclear cascade process.

The present analysis was carried out for the multiplicity distributions obtained from collisions of 360 GeV/c protons with aluminium and gold nuclei. Investigations of multiplicities are performed for various rapidity intervals, and also for the forward and backward hemispheres separately. This paper is organized as follows: in section 2 a brief description of the experimental data is given. The procedure for the analysis and the results are described in section 3, and comparisons to predictions of the Monte Carlo calculations are made in section 4, followed by a discussion. The conclusions are summarised in section 5.

2. Experimental Data

The data used in the present study were obtained by an exposure of the Rapid Cycling Bubble Chamber (RCBC) with the European Hybrid Spectrometer (EHS) to a 360 GeV/c proton beam (CERN experiment NA23). Nuclear targets were installed in the RCBC, filled with liquid hydrogen. The targets were made of aluminium (Al, mass number A=27) and gold (Au, A=197) foils with thicknesses of 1.6 mm and 0.3 mm, respectively. Details of the experimental set-up and data processing have been described elsewhere [15,19].

After scanning the film, 608 foil interaction candidates were measured and passed through the hybrid geometry reconstruction programs. We selected proton-nucleus events by applying the following criteria: 1)the reconstructed primary vertex must lie in the region corresponding to the position of foil targets, and 2)the reconstructed beam tracks in the RCBC and upstream beam chambers must match. 45 events of p-Al and 174 events of p-Au interactions were thus selected.

For this sample, the contamination of p-p interactions was estimated to be 1.5 % for p-Al and 7.5 % for p-Au interactions. Measurement and reconstruction losses were less than 1 % for p-Al and 5 % for p-Au collisions, respectively. Tracks with a momentum accuracy $\Delta p/p > 50$ % were rejected; such tracks were less than 2.5 % of all tracks found in the scanning. The average multiplicity and dispersion of multiplicity distributions are given in Table 1. Concerning particle identification, protons in the momentum range from 0.2 to 1.2 GeV/c were identified in the scanning, while the remaining particles were treated as pions.

3. Multiplicity Distributions

Hadron-nucleus collisions are generally understood as successive multiple collisions between a projectile and nucleons in a nucleus. Most of the particles produced in the forward hemisphere come directly from the fragmentation processes of the multiple collision, while those in the backward hemisphere include the particles produced by a different production process, the so-called intranuclear cascade [15].

Charged multiplicity distributions have been analysed separately in the forward and backward hemispheres, which are divided at laboratory rapidity y_{Lab} = 3.32 corresponding to a cms rapidity y_{cms} = 0 for proton-proton collisions at 360 GeV/c. We consider eight rapidity intervals of width Δy varying from 0.5 to 4.0, centred at y_{Lab} = 3.32 and extending to the forward and backward hemispheres. The value Δy = 4.0 corresponds to the full phase space. Figs. 1 and 2 show the multiplicity distributions for p-Al and p-Au collisions, respectively. The errors in the figures are statistical only.

The multiplicity distributions of charged particles in the selected rapidity intervals were fitted to the negative binomial distribution, eq.(1), with two free parameters. The fitted parameters, $\bar{n}$ and 1/k, are summarised in Table 2 for both hemispheres, where the χ^2 and the number of degrees of freedom NDF are given for each fit. The fit results are shown by the histograms in figs. 1 and 2.

The fitted parameters, $\bar{n}$ and 1/k, of the NBD as a function of rapidity interval are also displayed in fig. 3 for each target and for each hemisphere.

This analysis shows that the charged multiplicity distributions in various rapidity intervals for both Al and Au targets are well described with negative binomial distributions, i.e. eq.(1). We can summarise this analysis as follows;

- The A-dependence is clearly seen in the parameter $\bar{n}$.

- In the forward hemisphere, the parameter $\bar{n}$ increases linearly with the width of the rapidity interval chosen and then saturates in the region of large rapidity interval. On the other hand, the parameter 1/k is generally decreasing with increasing rapidity interval.

- In the backward hemisphere, the parameter $\bar{n}$ shows a linear increase proportional to the rapidity interval, and does not saturate. The parameter 1/k stays almost constant around 0.5-0.7. This behaviour of 1/k is remarkably different from the forward hemisphere. Furthermore, this feature cannot be found in other reactions, i.e. pp [2], e^+e^- [3] and μp interactions [4]. These characteristics in the backward hemisphere are connected with the existence of the intranuclear cascade process due to slow particles [14-15].

4. Comparison with Models and Discussion

4.1. Multi-chain Model for Hadron-Nucleus Collision

We have developed a Monte Carlo program MCMHA [16-17] based on the multi-chain model [18] in order to describe hadron-nucleus collisions. In this model, a hadron-nucleus collision is separated into two stages, one of which corresponds to successive multiple collisions between the projectile and nucleons inside the nucleus and the other to the fragmentation of hadronic chains stretched between them. We have also included the cascade process due to secondary particles inside the target nucleus.

The probability that a projectile hadron collides with ν-nucleons inside a target nucleus at a given impact parameter is calculated with the Glauber model [20]. At each collision the projectile hadron loses a fraction of its momentum according to a probability based on the multi-chain model [18].

After the first stage, the hadronic chains created by each collision between the projectile and nucleons fragment into pions and a recoil nucleon. The number of particles fragmented from a chain is determined by the KNO distribution for p-p collisions [6] with the average multiplicity determined by the energy available for the chain. The charge distribution of the fragmented pions is calculated by a statistical model satisfying charge conservation [21]. The rapidity of each pion is determined according to a probability distribution which is parameterised on the basis of experimental data for p-p collisions.

The hadrons can materialise only after a characteristic formation time [22]. We have introduced this formation zone concept into the chain fragmentation stage, and have adopted a proper time of 1 fm/c for the formation time of hadrons. According to the Lorentz time dilation, relativistic pions generally materialise outside the nucleus, while slow pions and recoil nucleons are formed inside the nucleus. Secondary particles thus formed propagate in the nucleus and may undergo cascade interactions with other nucleons. The cascade process produces grey particles knocked out of the nucleus. We have simulated the intranuclear cascade process under the assumption that the secondary particles formed in the nucleus interact with

nucleons only through the following processes;

$$\pi N \rightarrow \pi N,$$
$$\rightarrow \pi \Delta,$$
$$NN \rightarrow NN \text{ and}$$
$$\rightarrow N\Delta.$$

This approximation is appropriate because most of the particles which undergo cascade interactions have relatively low momenta.

4.2. Comparisons and Discussion

We compare the results of the Monte Carlo calculations with the experimental distributions. In fig. 1 and 2 solid lines represent the MCMHA calculations under the same conditions as the experimental data. All the MCMHA results are in good agreement with the experimental data and also with the NBD fitted lines for each hemisphere of both p-Al and p-Au collisions. In the same figure, the dashed lines show the results of the Lund Monte Carlo FRITIOF [23], in which the intranuclear cascade process is not included. For the forward hemisphere the Lund FRITIOF describes well the experimental results in each rapidity interval for both p-Al and p-Au collisions. On the other hand, for the backward hemisphere one can see some discrepancies from the experimental data. In particular, this behaviour appears distinctly in the high multiplicity region when the rapidity interval $|\Delta y|$ is larger than 3.5 for p-Al and 3.0 p-Au collisions respectively.

The clan model [9] has explained the origin of the NBD. The clan is considered as a cluster of particles with the same originator in its cascading decay process. In this model the average multiplicity $\bar{n}_c$ of decay particles in a clan is expressed

by the NBD parameters as follows;

$$\bar{n}_c = \frac{-b}{(1-b)\ln(1-b)} \qquad (3)$$

where

$$b = \bar{n}/(\bar{n}+k) \qquad (4).$$

The average number of produced clans is given by

$$\bar{N} = \bar{n}/\bar{n}_c, \qquad (5)$$

and their distribution is considered to be a Poissonian. Fig. 4 shows the dependences of $\bar{n}_c$ and $\bar{N}$ on the rapidity interval Δy in each hemisphere respectively.

Our experimental results are interpreted by the clan model as follows;

- In the forward hemisphere the average multiplicity of a clan is about 1.5 for both p-Al and p-Au collisions, and the rapidity width of a clan seems to be small because $\bar{n}_c$ is almost constant in the whole rapidity interval.

- The average multiplicity of a clan in the backward hemisphere is appreciably larger than that in the forward hemisphere. The increase of $\bar{n}_c$ with Δy points out that the clans in the backward hemisphere have a larger rapidity width. The value of $\bar{n}_c$ in the backward hemisphere shows a clear A-dependence.

- The average number of clans produced in the forward hemisphere has a little A-dependence. Furthermore, the number of clans produced in the forward hemisphere is systematically larger than in the backward hemisphere. This puzzling result has been observed in 200 GeV/c p-Ar and p-Xe

collisions [14].

5. Summary

We have analysed multiplicities of all charged particles produced in collisions of 360 GeV/c proton with aluminium and gold targets.

Multiplicity distributions of particles produced in various rapidity intervals are quite well explained by a negative binomial distribution for each hemisphere when the fitting has been limited to either the forward or the backward hemisphere. A description of the multiplicity distribution with the negative binomial distribution has been already done in other elementary interactions and 200 GeV/c proton-nucleus collisions. We have confirmed the observation in 200 GeV/c p-nucleus collisions in 360 GeV/c p-Al and p-Au collisions.

We can interpret the multiplicity distributions remarkably well with the Monte Carlo program MCMHA. On the other hand, the Lund Monte Carlo FRITIOF, which does not take into account intranuclear cascades, does well not describe the multiplicity distribution particularly in the backward hemisphere. This fact points out that the intranuclear cascade process is very important in the backward hemisphere.

We have also interpreted the experimental results in the framework of the clan model and have obtained similar results to those of 200 GeV/c proton-argon and xenon collisions. The puzzling result about the average number of clans produced in the

forward and backward hemispheres could be understood by considering the intranuclear cascade process.

Acknowledgements

We gratefully acknowledge the efforts of the scanning and measuring personnel of the collaborating institutions for their painstaking counting of tracks and measurement of the complex nuclear interactions. We wish to thank Drs. H.Sumiyoshi and N.Suzuki for useful discussions. We are indebted to Mr. S.Yamazaki for the development of the Monte Carlo program MCMHA.

References

[1] G.J.Alner et al, Phys. Lett. 160B (1985), 193
G.J.Alner et al, Phys. Lett. 160B (1985), 199
G.J.Alner et al, Phys. Lett. 167B (1986), 476

[2] M.Adamus et al, Phys. Lett. 177B (1986), 239

[3] M.Derrick et al, Phys. Lett. 168B (1986), 299

[4] M.Arneodo et al, Z. Phys. C 35 (1987), 335

[5] Z.Koba, H.B.Nielsen and P.Olesen, Nucl. Phys. B40 (1972), 317

[6] P.Slattery, Phys. Rev. Lett. 29 (1972), 1624

[7] N.Suzuki, Prog. Theor. Phys. 51 (1974), 1629

[8] A.Giovannini et al, Nuovo Cimento A24 (1974), 421

[9] A.Giovannini and L.Van Hove, Z. Phys. C 30 (1986), 391

[10] E.D.Malaza and B.R.Webber, Nucl. Phys. B267 (1986), 702

[11] A.Białas, I.Derado and L.Stodolsky, Phys. Lett. 156B (1985), 421

[12] K.Fiałkowski, Phys. Lett. 169B (1986), 436

[13] A.Białas and A.Szczerba, Jagellonian University preprint TPJU 18-86

[14] F.Dengler et al, Z. Phys. C 33 (1986), 187

[15] J.L.Bailly et al, Z. Phys. C 35 (1987), 301

[16] Y.Iga, R.Hamatsu, S.Yamazaki and H.Sumiyoshi, Prog. Theor. Phys. 77 (1987), 376

[17] Y.Iga, R.Hamatsu, S.Yamasaki and H.Sumiyoshi, Preprint MGJC-HE-87-1
To be published to Z. Phys. C

[18] K.Kinoshita, A.Minaka and H.Sumiyoshi, Prog. Theor. Phys. 63 (1980), 928
S.Datè, M.Gyulassy and H.Sumiyoshi, Phys. Rev. D32 (1985), 619

[19] J.L.Bailly et al, Z. Phys. C 23 (1984), 205

[20] R.J.Glauber, Lectures in Theoretical Physics, Vol.1 p315, ed. W.E.Britin and L.G.Dunham, New York, Interscience (1959)

[21] S.J.Orfanidis and V.Rittenberg, Nucl. Phys. B59 (1973), 570

[22] R.Annishetty, P.Kohler and L.McLerran, Phys. Rev. D22 (1980), 2793

[23] B.Anderson, G.Gustafson and B.Nilsson-Almqvist, Nucl. Phys. B281 (1987), 289 ; B.Nilsson-Almqvist and E.Stenlund, Lund preprint LUIP 8507/LU-TP 85-7, 1985

Table Captions

Table 1. The average multiplicity and the dispersion of multiplicity distributions for p-Al and p-Au collisions. Both values obtained by the scanning and by the numbers of measured and selected tracks are given.

Table 2. Parameters of negative binomial distributions fitted to the charged multiplicity distributions. The χ^2 and the number of degrees of freedom for various rapidity intervals Δy are also given. a: p-Al forward hemisphere, b: p-Al backward hemisphere, c: p-Au forward hemisphere and d: p-Au backward hemisphere.

		Scan Multiplicity	Selected track Multiplicity
Al	<n>	17.7 ± 1.6	17.1 ± 1.5
	D	10.5 ± 1.3	10.0 ± 1.2
Au	<n>	27.1 ± 1.3	25.1 ± 1.2
	D	17.2 ± 1.0	15.8 ± 0.9

Table 1.

Δy		$\bar{n}$	1/k	χ^2/NDF
0.5	Ia	1.32 ± 0.25	0.47 ± 0.44	0.6/2
	Ib	2.19 ± 0.48	0.74 ± 0.39	0.6/3
	Ic	2.00 ± 0.17	0.32 ± 0.10	13.8/7
	Id	2.01 ± 0.17	0.56 ± 0.04	10.6/8
1.0	Ia	2.77 ± 0.43	0.59 ± 0.29	1.5/5
	Ib	3.64 ± 0.94	0.82 ± 0.41	0.6/4
	Ic	3.58 ± 0.16	0.47 ± 0.06	15.8/11
	Id	4.20 ± 0.30	0.62 ± 0.10	9.5/14
1.5	Ia	3.85 ± 0.60	0.51 ± 0.18	3.3/4
	Ib	4.97 ± 0.67	0.51 ± 0.21	2.1/5
	Ic	4.95 ± 0.30	0.33 ± 0.10	26.8/13
	Id	6.88 ± 0.56	0.57 ± 0.08	8.8/20
2.0	Ia	4.70 ± 0.57	0.31 ± 0.15	6.5/6
	Ib	6.93 ± 0.80	0.50 ± 0.20	0.5/4
	Ic	6.00 ± 0.28	0.20 ± 0.05	20.3/15
	Id	9.32 ± 0.74	0.56 ± 0.09	27.1/25
2.5	Ia	5.37 ± 0.56	0.27 ± 0.11	2.5/3
	Ib	8.84 ± 1.66	0.49 ± 0.19	2.2/4
	Ic	6.53 ± 0.31	0.19 ± 0.05	19.2/14
	Id	11.92 ± 1.16	0.59 ± 0.02	37.1/31
3.0	Ia	5.80 ± 0.53	0.21 ± 0.10	4.7/3
	Ib	10.42 ± 2.33	0.57 ± 0.19	2.2/4
	Ic	6.95 ± 0.33	0.16 ± 0.04	31.7/15
	Id	14.81 ± 1.93	0.63 ± 0.03	54.2/37
3.5	Ia	5.62 ± 0.58	0.19 ± 0.10	4.6/3
	Ib	11.91 ± 1.72	0.61 ± 0.17	0.6/5
	Ic	7.21 ± 0.29	0.15 ± 0.05	35.0/15
	Id	18.52 ± 1.31	0.64 ± 0.06	56.6/46
4.0	Ia	6.55 ± 0.70	0.25 ± 0.12	2.4/2
	Ib	12.68 ± 2.33	0.64 ± 0.20	0.7/5
	Ic	7.14 ± 0.31	0.15 ± 0.05	30.9/15
	Id	19.17 ± 0.99	0.62 ± 0.07	56.6/42

Table 2

Figure Captions

Fig. 1. Charged multiplicity distributions for p-Al collisions for various rapidity intervals a) in the forward, b) in the backward hemispheres. (as defined in the text). The histograms show the negative binomial distributions fitted to the data points. The solid and dashed lines show the predictions of MCMHA and Lund FRITIOF, respectively. The ordinates of the distribution for $|\Delta y| = 4.0$ have not been rescaled, but each consecutive one is scaled down by an additional factor of 10. The points with the lowest values and the largest errors are not shown because of the logarithmic scale.

Fig. 2. Charged multiplicity distributions for p-Au collisions.

Fig. 3. The fitted values of the NBD parameters as a function of the rapidity interval Δy for charged multiplicity distributions. a), b) for $\bar{n}$, and c), d) for $1/k$ for the forward and backward hemispheres respectively. Circles and diamonds show the values for p-Al and p-Au collisions respectively.

Fig. 4. The deduced parameters of the clan model. a), b) for the average decay multiplicity $\bar{n}_c$ of a clan, and c), d) for the average clan multiplicity $\bar{N}$ as a function of the rapidity interval Δy for charged particles. a), c) for the forward hemisphere, and b), d) for the backward hemisphere.

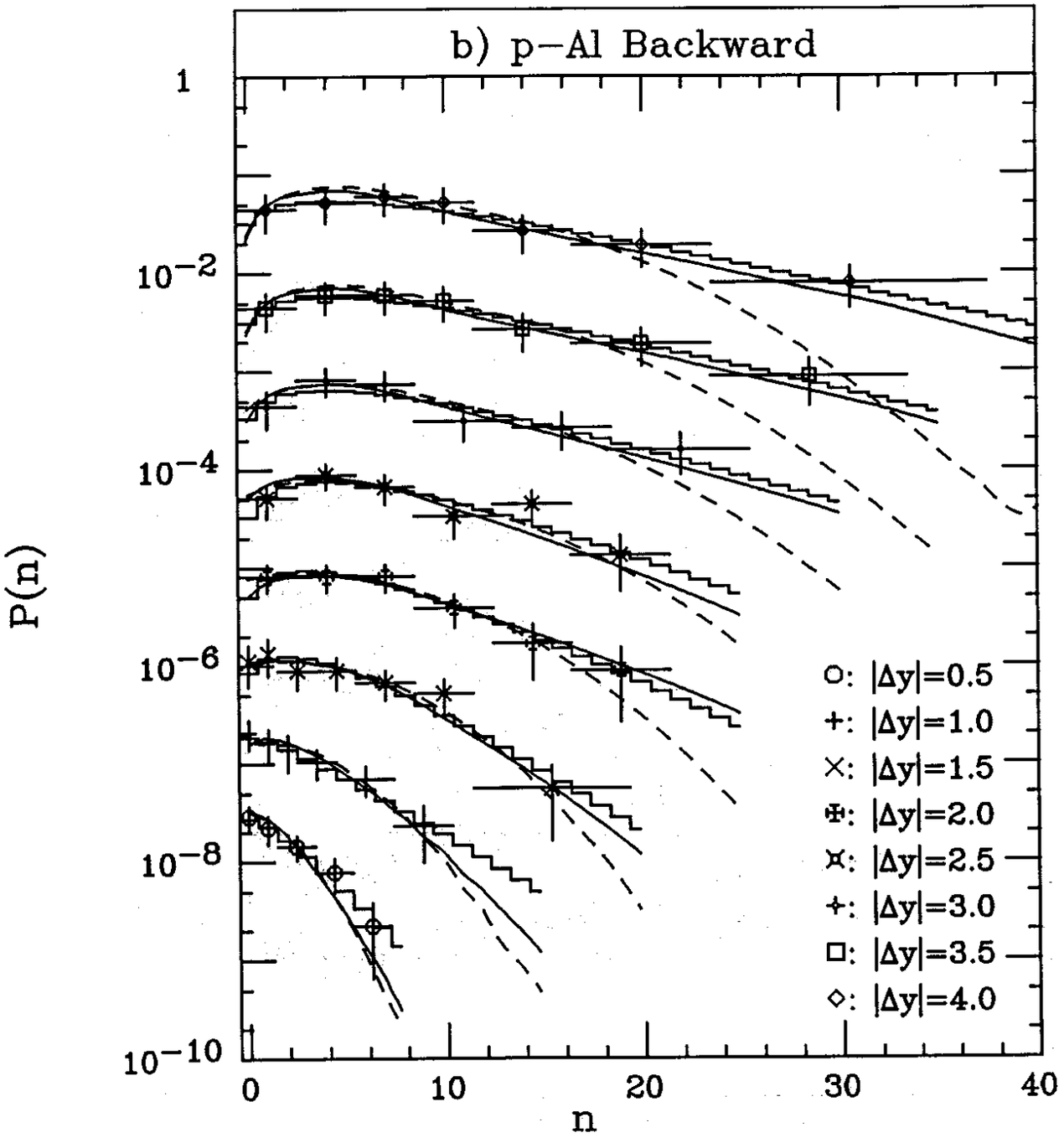
b) p−Al Backward
P(n)
n
1
10^{-2}
10^{-4}
10^{-6}
10^{-8}
10^{-10}
0
10
20
30
40
○: |Δy|=0.5
+: |Δy|=1.0
×: |Δy|=1.5
⊕: |Δy|=2.0
⊠: |Δy|=2.5
+: |Δy|=3.0
□: |Δy|=3.5
◇: |Δy|=4.0

fig. 1

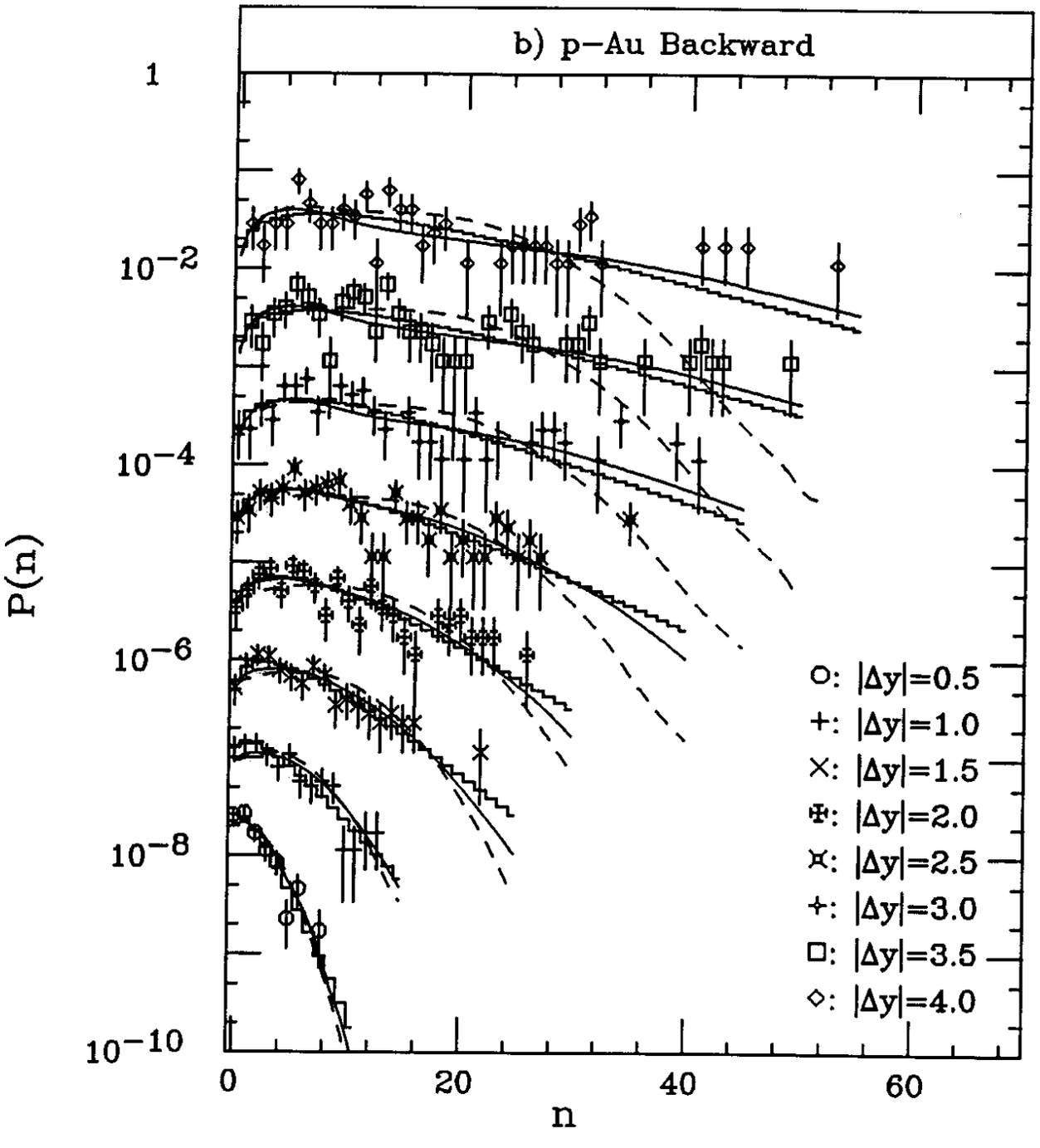
b) p−Au Backward
1
10^{-2}
10^{-4}
10^{-6}
10^{-8}
10^{-10}
P(n)
0
20
40
60
n
○: |Δy|=0.5
+: |Δy|=1.0
×: |Δy|=1.5
✠: |Δy|=2.0
✠: |Δy|=2.5
+: |Δy|=3.0
□: |Δy|=3.5
◇: |Δy|=4.0

fig. 2

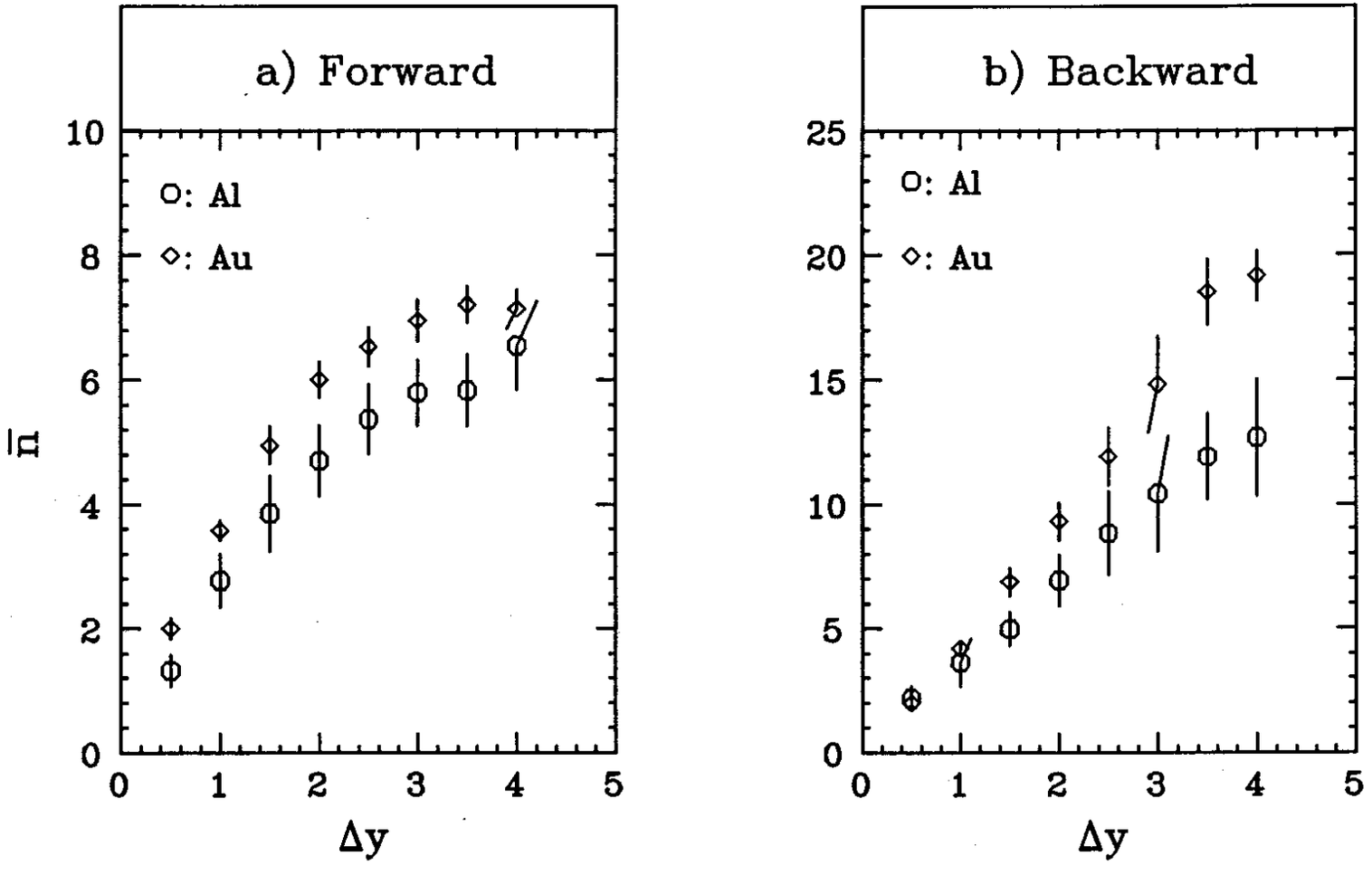
a) Forward
b) Backward
○: Al
◇: Au
$\bar{n}$
Δy
0
1
2
3
4
5
0
2
4
6
8
10
0
5
10
15
20
25

fig. 3

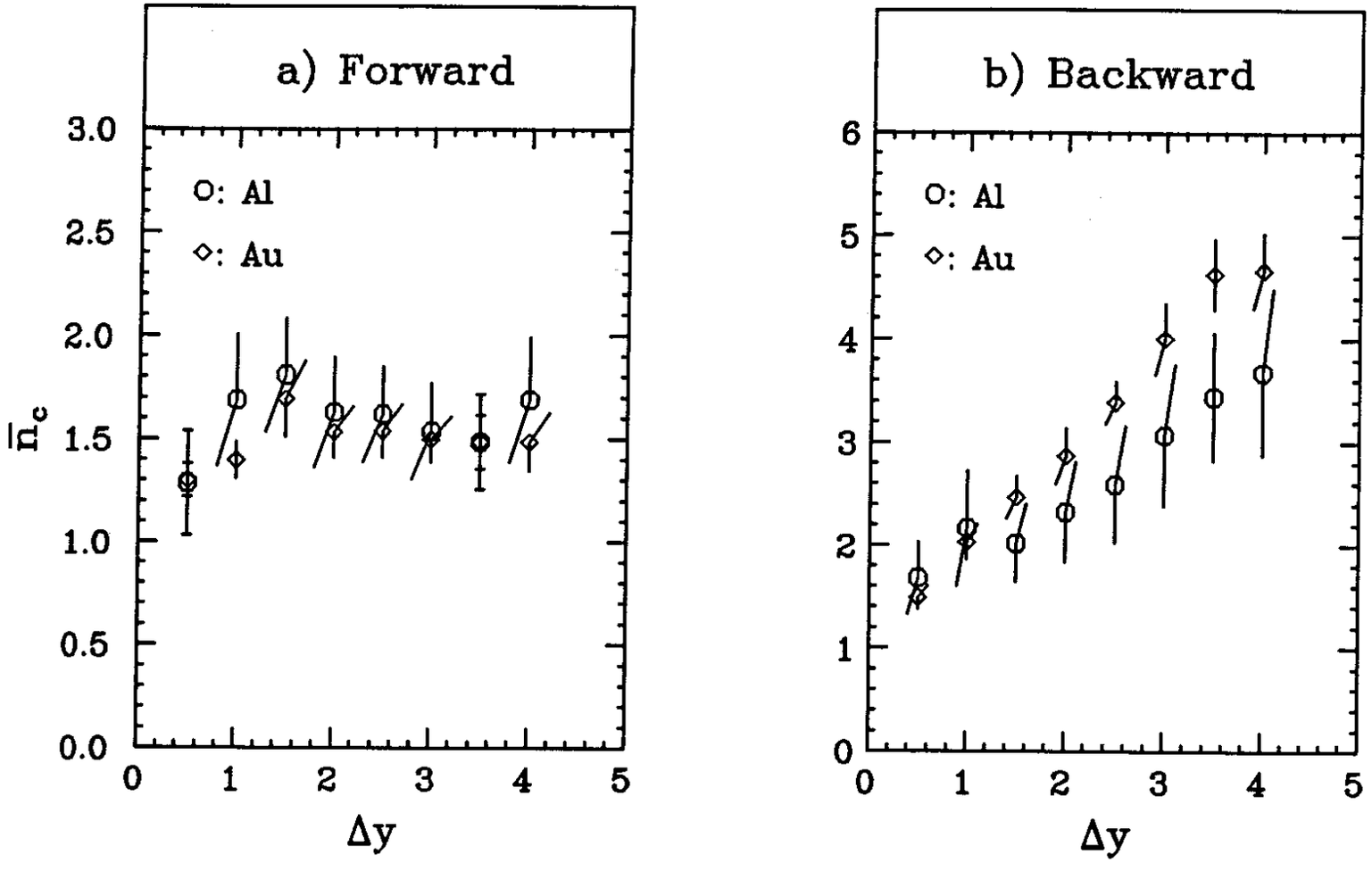

fig. 4